JOURNAL OF APPLIED ELECTROCHEMISTRY 23 (1993) 790–800

Mechanism of the cathode reaction in sodium–ferrous chloride secondary cells

J. COETZER

Zebra Power Systems, P.O. Box 7255, Hennopsmeer 0046, South Africa

G. D. WALD, S. W. ORCHARD*

Centre for Applied Chemistry and Chemical Technology, Department of Chemistry, University of the Witwatersrand, Private Bag 3, Wits 2050, South Africa

Received 7 July 1992; revised 3 October 1992

The electrochemical behaviour of iron electrodes in molten $AlCl_3$: NaCl saturated with NaCl has been studied in the temperature range 175–400 °C. The results suggest that the electrochemical oxidation of iron occurs most readily in the presence of solid NaCl on the electrode, and that solid $FeCl_2$ is reduced more readily than dissolved Fe(II) in this electrolyte. A predominantly solid state mechanism is thus indicated for the charge and discharge of $FeCl_2$ cathodes used in high energy sodium cells which operate near 250 °C. Results obtained in a cell containing no liquid electrolyte provide additional support for a solid state mechanism. The participation of the solid compound Na_6FeCl_8, which was previously reported to be an intermediate in the charge and discharge processes, has been confirmed, but it does not appear to have any significant adverse effect on the electrochemical performance. At high temperatures (300–400 °C) dissolved reagents and products can contribute increasingly to the cathode reaction mechanism.

1. Introduction

High energy density secondary sodium cells in which the cathode reagent is a transition metal chloride have been reported in recent years [1–11]. The preferred metal chlorides are $FeCl_2$ and $NiCl_2$ [1–4, 7, 8], although other transition metals have also been studied [5, 11–13]. In the case of $FeCl_2$, for example, the overall cell reaction is

$$2Na(l) + FeCl_2(s) \rightleftharpoons Fe(s) + 2NaCl(s) \quad (1,-1)$$

The cathodes are fabricated in the discharged state by sintering a mixture of Fe and NaCl powders, a stoichiometric excess of the former being used in order to achieve adequate electronic conductivity in the fully charged cathode. An electrolyte of molten $AlCl_3$: NaCl floods the porous cathode, while β''-alumina solid electrolyte separates the anode and cathode compartments.

Sodium ions migrate between anode and cathode during cell operation; the cathode reaction can thus be written as

$$FeCl_2(s) + 2Na^+ + 2e^- \rightleftharpoons Fe(s) + 2NaCl(s) \quad (2,-2)$$

While solid $FeCl_2$ and NaCl are undoubtedly present in the cathode it is not immediately apparent whether they react directly according to Reactions 2, −2, or whether they first dissolve to form intermediates, for example $FeCl_4^{2-}$ and Cl^-, which then react. Some relevant information on this question is available from earlier work. First, there is good evidence that the cathode process during normal operation at 250 °C (a suitable temperature for Na–$FeCl_2$ cells [4]) involves the intermediate solid compound Na_6FeCl_8 [2]. Thus Reactions 2,−2 should be seen as the net result of the separate reactions, 3,−3 and 4,−4, as follows:

$$4FeCl_2(s) + 6Na^+ + 6e^- \rightleftharpoons 3Fe(s) + Na_6FeCl_8(s) \quad (3,-3)$$

$$Na_6FeCl_8(s) + 2Na^+ + 2e^- \rightleftharpoons Fe(s) + 8NaCl(s) \quad (4,-4)$$

Secondly, Ratnakumar and coworkers [11] have suggested that the reduction of both $NiCl_2$ and $FeCl_2$ involves the diffusion of metal ions across solid product layers.

This paper reports on a variety of experiments relating to the behaviour of the Fe(II)/Fe couple in these cells. Some of these are directly relevant to the question of whether the mechanism involves solids only, or whether solution phase reagent and product species, other than Na^+, are also important; the results are reported in this paper.

2. Experimental details

Aluminium chloride (Fluka, puriss., anhydrous, iron-

*Author to whom correspondence should be addressed at: 1701 224th Court N.E., Redmond, WA 98053, USA.

0021-891X

free) and sodium chloride (Merck, analytical grade, 99.5%) were purified and mixed to give NaCl-saturated melts as described previously [12]. All $AlCl_3$: NaCl melts used in this work were saturated with NaCl, and this electrolyte will be referred to simply as the molten salt. Iron (II) chloride (Cerac, 99.99%) was used as received.

The solubility of $FeCl_2$ in NaCl-saturated $AlCl_3$: NaCl was determined by first saturating the melt with $FeCl_2$ in the presence of excess solid NaCl. The mixture was agitated intermittently over several days during this process. The solid phases Na_6FeCl_8, Na_2FeCl_4 and $Na_2Fe_3Cl_8$ are all known [6]; sufficient excess NaCl was used to ensure that only the first of these could be present at equilibrium. After allowing all solids to settle out, an aliquot of the solution was removed in a preweighed disposable Pyrex pipette. After cooling and weighing of the pipette and contents, it was transferred to a volumetric flask, and water was added. The solution was analysed for iron by atomic absorption spectrophotometry at 248.3 nm.

Most electrochemical measurements were carried out using about 30 g of melt in a Pyrex cell fitted with 'Ace-Thred' adapters and Teflon bushings and ferrules to hold three electrodes. The lower part of the cell fitted into a furnace, so that the Teflon components were well above the heated zone. Temperature control of the melt was within 0.1 °C. Iron wire working electrodes were of diameter approximately 0.5 mm (Johnson Matthey, puratronic), and were immersed in the melt to a depth of approximately 5 mm, to give active electrode areas of about $0.08 \pm 0.02\,cm^2$. Before being used for electrochemistry, the iron was cleaned by immersion in boiling 1 : 1 HCl. The counter and reference electrodes were aluminium wires in housings with fine porosity sintered Pyrex discs linking them to the bulk melt. NaCl-saturated melts were maintained at both the counter and reference electrodes by having small amounts of solid NaCl in contact with the melt in the fritted housings; except where indicated otherwise, all potentials in this paper are reported with respect to aluminium in the saturated melt.

Working electrodes of either tungsten or Fe/NaCl sinters were also used in some experiments. The tungsten electrode was made by sealing a 1.0 mm diameter wire in Pyrex tubing, cutting through the seal perpendicularly, and polishing the exposed disc with successively finer grades of emery paper and alumina powder to the desired finish. Porous Fe/NaCl electrodes were made by cosintering the finely divided solids in a graphite mould, using an embedded tungsten wire as the current collector [13].

A two-electrode cell was constructed for studies using NaCl as a solid electrolyte. The cell had a solid, insulating body through which was drilled a 6.35 mm diameter hole. Two close fitting cylindrical metal rods placed end to end in this hole served as the electrodes. Their adjacent faces were cut square and polished to a mirror finish. One rod was always iron; the second rod terminated with a disc of either iron, nickel or copper, as appropriate. The rods were partially threaded and were held in place by nuts which fitted into recesses in the insulating body of the cell. The small gap (~ 0.1 mm) between the electrode faces was filled with finely ground NaCl ($< 20\mu m$). Open circuit voltages of this cell were measured using a Fluke 8810A meter with an input impedance of $> 1000\,M\Omega$.

Electrochemistry was carried out in either a purge-type glove box under nitrogen or in a high integrity recirculating glove box (Faircrest) under argon. Cyclic voltammograms (CVs) were obtained using an E.G. and G. Princeton Applied Research model 362 potentiostat linked to an *XY*-recorder (Watanabe WX451). Chronopotentiometry was carried out using the potentiostat in galvanostat mode, controlled and monitored by an IBM PC XT-compatible computer via an IBM data acquisition and control adapter card.

3. Results and discussion

3.1. *Reagent solubility*

It is informative to first consider some simple calculations relating to the solubilities of reagents and products in the molten $AlCl_3$: NaCl electrolyte. An NaCl-saturated melt can be considered to be a saturated solution of NaCl in $NaAlCl_4$ (i.e. in a 1 : 1 melt). Torsi and Mamantov [14] give the solubility at 250 °C as $0.10\,mol\,kg^{-1}$ (~ 0.16 M). During normal cell operation, the electrolyte remains basic, i.e. $AlCl_3$: NaCl < 1 : 1. Thus, at most, 0.16 mol of dissolved NaCl per dm^3 of melt is available to participate in cell charging, Reaction −1. A representative cathode (85% porosity, 40% utilization of Fe [2]) in the discharged state contains 4.9 mol of solid NaCl per dm^3 of pore volume; thus, not more than 3.3% of the original NaCl reagent is in solution at any given time. At a typical charging rate, 10 h, this dissolved NaCl is depleted in about 20 min. For the discharge process, a similar calculation can be performed, based on the solubility of $FeCl_2$ in NaCl-saturated $AlCl_3$: NaCl. The results of solubility measurements of $FeCl_2$ in the NaCl-saturated electrolyte are summarized in Fig. 1. The solubility of $FeCl_2$ at 250 °C is $0.028\,mol\,kg^{-1}$ (~ 0.047 M), so that about 1.9% of the $FeCl_2$ in a fully charged cell is in solution at saturation. At a 3 h discharge rate, this is consumed in only 3.4 min.

The amounts of dissolved $FeCl_2$ and NaCl at 250 °C are thus small in relation to the amounts of the solid salts present in a cathode. However, this does not rule out charge and discharge mechanisms involving dissolution of the reagents prior to electron transfer, followed by precipitation of the products. The slow rate of dissolution of NaCl in nearly saturated $AlCl_3$: NaCl has been noted by Osteryoung and coworkers [15]; this tends to militate against a

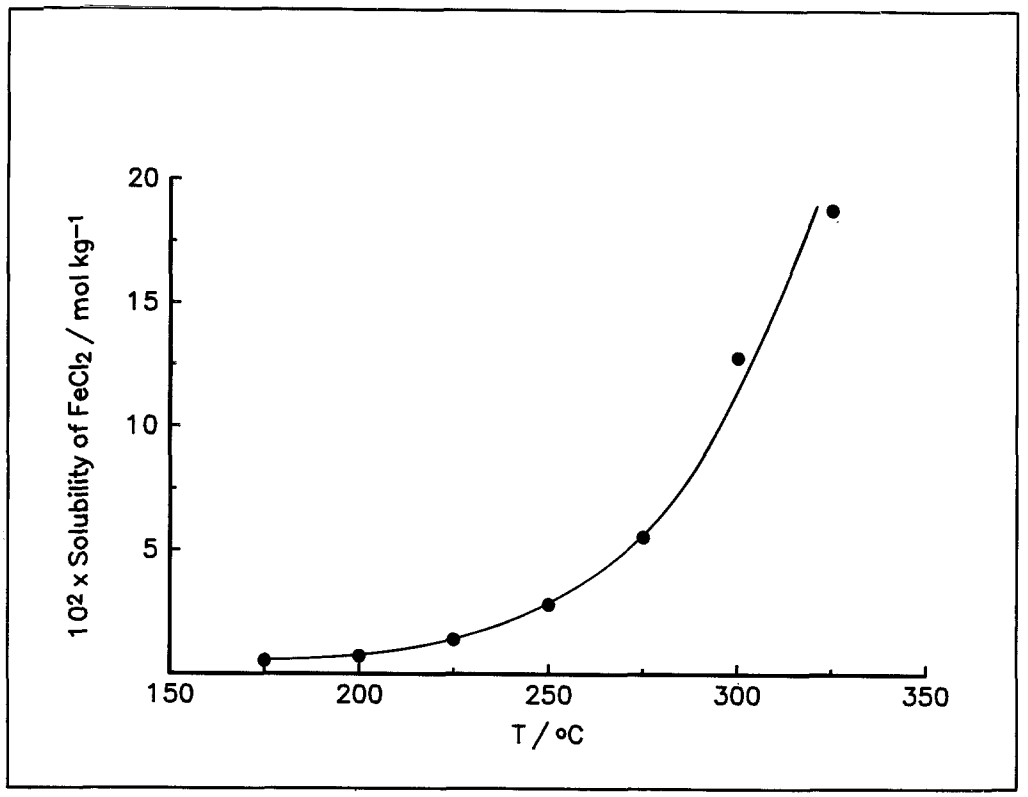

Fig. 1. Solubility of $FeCl_2$ against temperature in an NaCl-saturated melt.

charging mechanism involving dissolved NaCl in the form of Cl^-.

As the temperature increases above 250 °C, the solubilities of both NaCl and $FeCl_2$ increase significantly. For NaCl at 300 °C it is 0.15 mol kg^{-1} (~ 0.24 M) [14], while for $FeCl_2$ it is 0.128 mol kg^{-1} (~ 0.20 M), the latter figure being over four times the value at 250 °C. As the temperature increases the rates of dissolution of these salts are also expected to increase. Such solubility effects are clearly seen in some of the CV and chronopotentiometric data presented later. It is clear that dissolved reagents play an increasingly important role, relative to reagents in the solid state, as the cathode operating temperature increases.

3.2. *Cyclic voltammetry*

The CV data show a marked dependence on temperature. In particular, the general features of low temperature CVs (175–250 °C) are significantly different to those at higher temperatures (275–400 °C). The CV data for the two temperature regimes are thus considered separately. Figure 2 shows CVs obtained during continuous cycling of an iron wire working electrode in a NaCl-saturated melt at 250 °C. On the initial anodic sweep a fairly broad peak is seen at about 0.87 V. In subsequent cycles this peak is largely replaced by a new, narrower and higher peak which develops at a less anodic potential, about 0.80 V. During continuous cycling, both the anodic and the cathodic peaks grow until a steady state is approached. At temperatures below 250 °C this growth is also seen, with a longer period of cycling needed to achieve the steady state pattern. (Similar behaviour, apart from the fine structure, has also been noted for cobalt in the same melt [12].) The anodic process is undoubtedly the oxidation of Fe to Fe(II). (The $FeCl_3(s)/FeCl_2(s)$ couple can be calculated to lie about 1.3 V anodic of the $FeCl_2(s)$/Fe couple [16], and need not be considered in the potential range of the experiments.) Before the first sweep, there is no solid NaCl (or $FeCl_2$) on the surface of the electrode. Any Cl^- required for oxidation steps such as Reac-

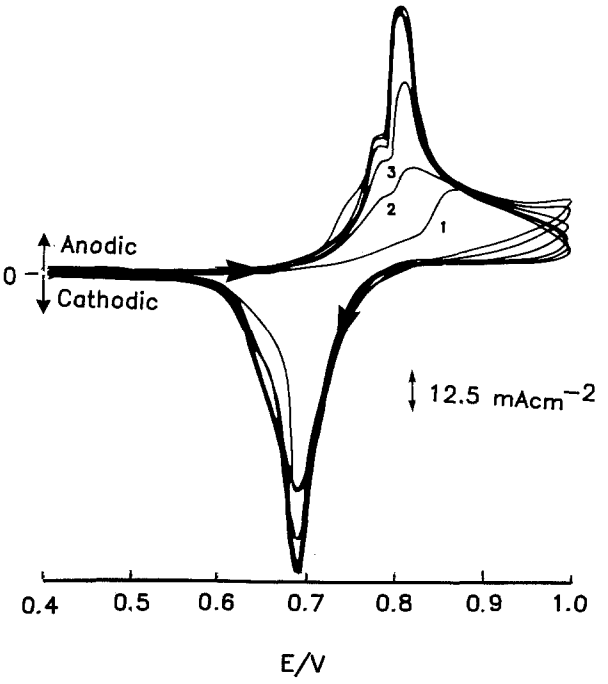

Fig. 2. Continuous CV of an iron wire in the molten salt at 250 °C, sweep rate 50 mV s^{-1}. Integers indicate cycle numbers.

tions 5 and 6 would of necessity come from solution:

$$Fe(s) + 2Cl^-(melt) \rightarrow FeCl_2(s) + 2e^- \quad (5)$$

$$Fe(s) + 4Cl^-(melt) \rightarrow FeCl_4^{2-}(melt) + 2e^- \quad (6)$$

Subsequent cathodic reduction of either of these products liberates Cl^- at the electrode surface in a melt already nearly saturated with NaCl. Saturation occurs, NaCl precipitates on the electrode, and is available as a source of Cl^- on subsequent anodic sweeps. The improved kinetics on the second and subsequent sweeps is striking (greater anodic peak current I_{pa}, less anodic peak potential E_{pa}), and suggests a change of mechanism, from one involving dissolved Cl^- on the first sweep to one involving solid NaCl on subsequent sweeps.

Both the first-cycle and the steady state anodic peaks have been compared to theoretical peak shapes calculated from the expressions of Nicholson and Shain [17, 18] (for electroactive reagents and products in solution) and Schiffrin [19] (for an electroactive solute forming a solid product). The experimental steady state peak is far narrower and higher than those predicted by either theory. The first-cycle peak most closely resembles that of Schiffrin's theory, but the presence of the shoulder precludes the possibility of good matching of the peak shapes. Peak shapes did show small differences from one melt preparation to another, although the main features were always present. This variability is possible due to differences in the levels of oxide, a ubiquitous impurity in these melts.

When the steady state is reached, the anodic and cathodic peak areas are very similar, showing that the products of anodic oxidation remain in the vicinity of the electrode and are reduced on the subsequent cathodic sweep. The matter of coulombic reversibility is addressed below.

Ratnakumar and coworkers [11] have reported cyclic voltammograms of an iron wire, though their work was apparently done in a 1 : 1 melt rather than an NaCl-saturated one, and was limited to 220 °C. They observed some fine structure in the peaks, but did not refer to any change in character of the peaks during continuous cycling. The steady state CV in Fig. 2 is very similar to the CV reported by Ratnakumar, and the separation between the oxidation and reduction peaks of about 110 mV is consistent with their value of 85 mV, which was measured at a lower sweep rate.

In both the Randles–Sevcik [18] and Schiffrin [19] expressions, the peak current (I_p) is proportional to the square root of the sweep rate (ν). Where other parameters are equal, the Schiffrin expression predicts the slope of the I_p against $\nu^{0.5}$ plot to be about 37% greater than does the Randles–Sevcik equation. Plots of the I_p against $\nu^{0.5}$ for the first anodic sweep were reasonably linear, but did not pass accurately through the origin (Fig. 3). However, this may have been due in part to error in determining the baseline correction, resulting from the presence of the shoulder on the peak. The slopes increase sharply with increasing temperature, which is consistent with the increasing concentration of free Cl^- available for Reactions 5 and 6 [14], the increase in the diffusion coefficient of this ion, and improved electron transfer kinetics. However, in

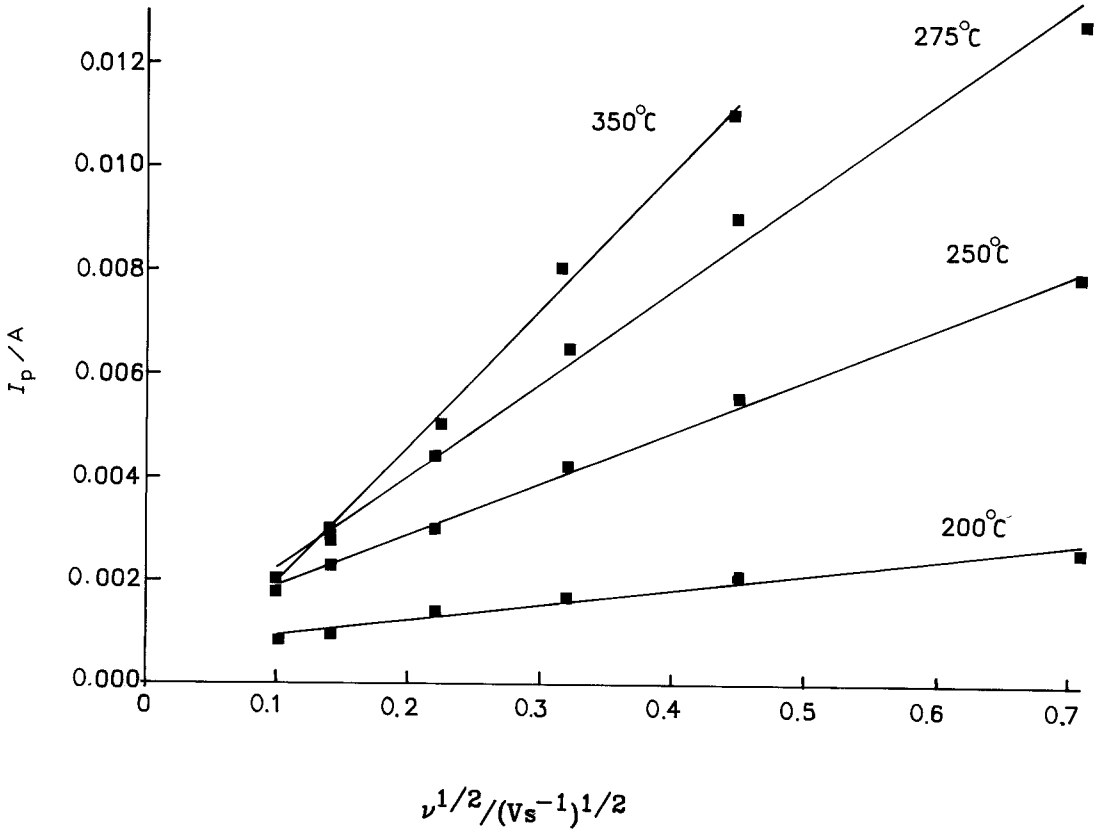

Fig. 3. Plots of I_p against $\nu^{0.5}$ for the first anodic sweep on an iron wire electrode in the molten salt at various temperatures.

view of the various uncertainties (in particular the exact active surface area of the working electrode) it is probably not justified to attempt to draw more quantitative conclusions from these plots.

Both the anodic and cathodic peaks in Fig. 2 exhibit some fine structure, although it is poorly resolved. Improved resolution is obtainable by suitable adjustment of the potential limits used. By reducing the anodic limit, more structure can be seen in the cathodic scan, and vice versa. Examples are shown in Fig. 4. The procedure followed was to cycle the electrode until the steady state voltammogram

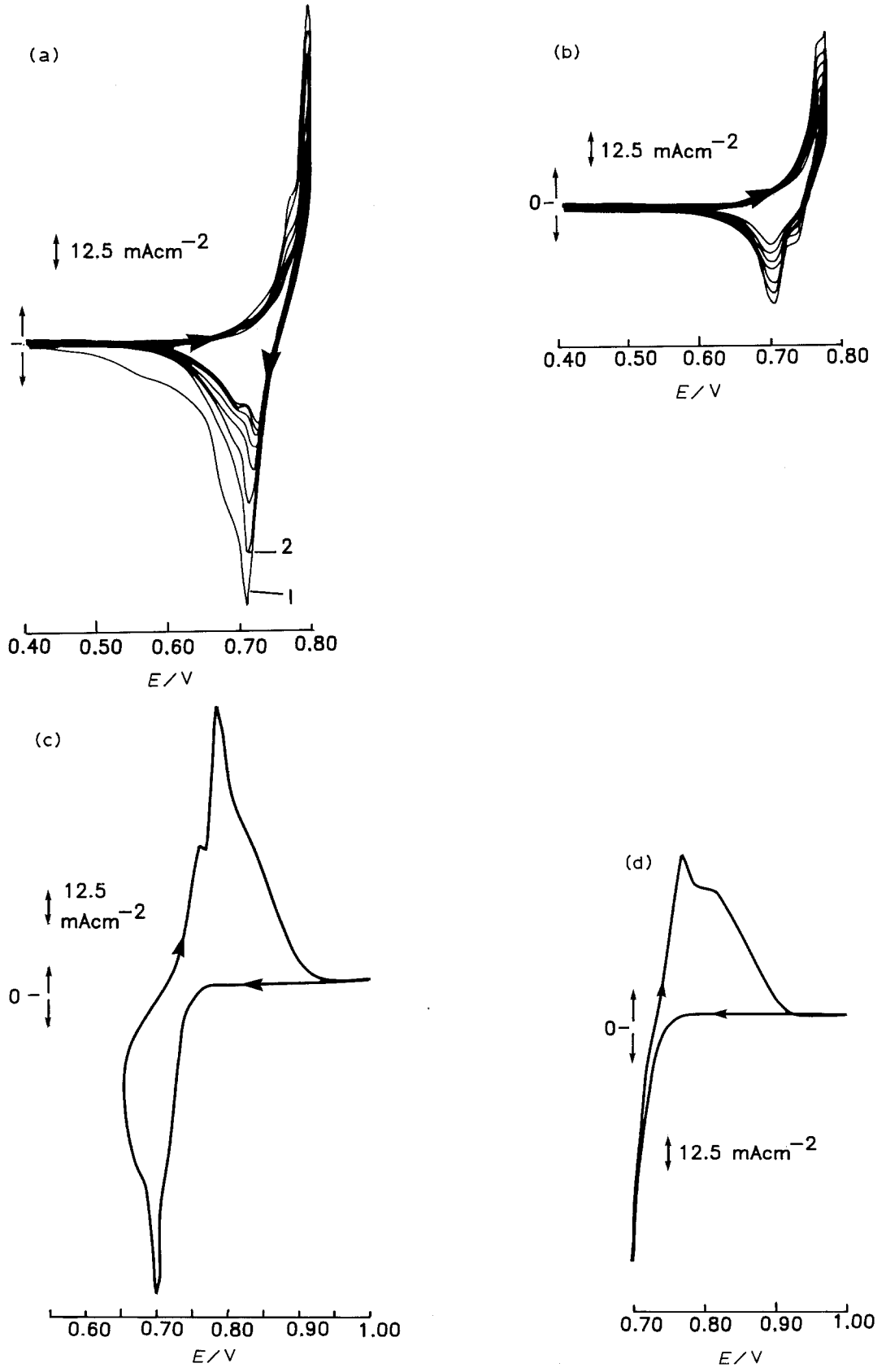

Fig. 4. CVs at 250 °C with restricted potential limits; normal limits were 0.400 V (cathodic) and 1.000 V (anodic). (a) Anodic limit 0.800 V; (b) anodic limit 0.778 V; (c) cathodic limit 0.650 V; (d) cathodic limit 0.700 V.

(Fig. 2) was obtained, then to change one of the potential limits and record the subsequent CVs, without interrupting the cycling process. From Fig. 4(a) and (b) it is clear that the main cathodic peak in Fig. 2 actually consists of two sharp and closely spaced peaks separated by 20–40 mV, depending on conditions. Figure 4(c) displays a similar, sharp anodic doublet, with a separation of about 25 mV, while Fig. 4(d) shows one of the doublet peaks in addition to a broader anodic peak at more anodic potentials. Figure 4(a) also shows a broad cathodic peak on the first cycle, at more negative potentials than the sharp peaks.

Enhanced resolution of CV peaks could also be achieved by cycling an inert electrode in a melt saturated with $FeCl_2$. Figure 5 shows examples, obtained with a tungsten working electrode at 250 °C. These CVs commenced with a cathodic going sweep, since only dissolved $FeCl_2$ (probably in the form of a chloride-rich complex such as $FeCl_4^{2-}$ [20]) is initially available for reaction. In a melt free of $FeCl_2$, the tungsten electrode showed very small CV currents in the potential range of interest (Fig. 5(a)). With $FeCl_2$ present, the cathodic peak on the first cycle (Fig. 5(b)) was smaller, broader and displaced cathodically compared to the peak seen on sub-

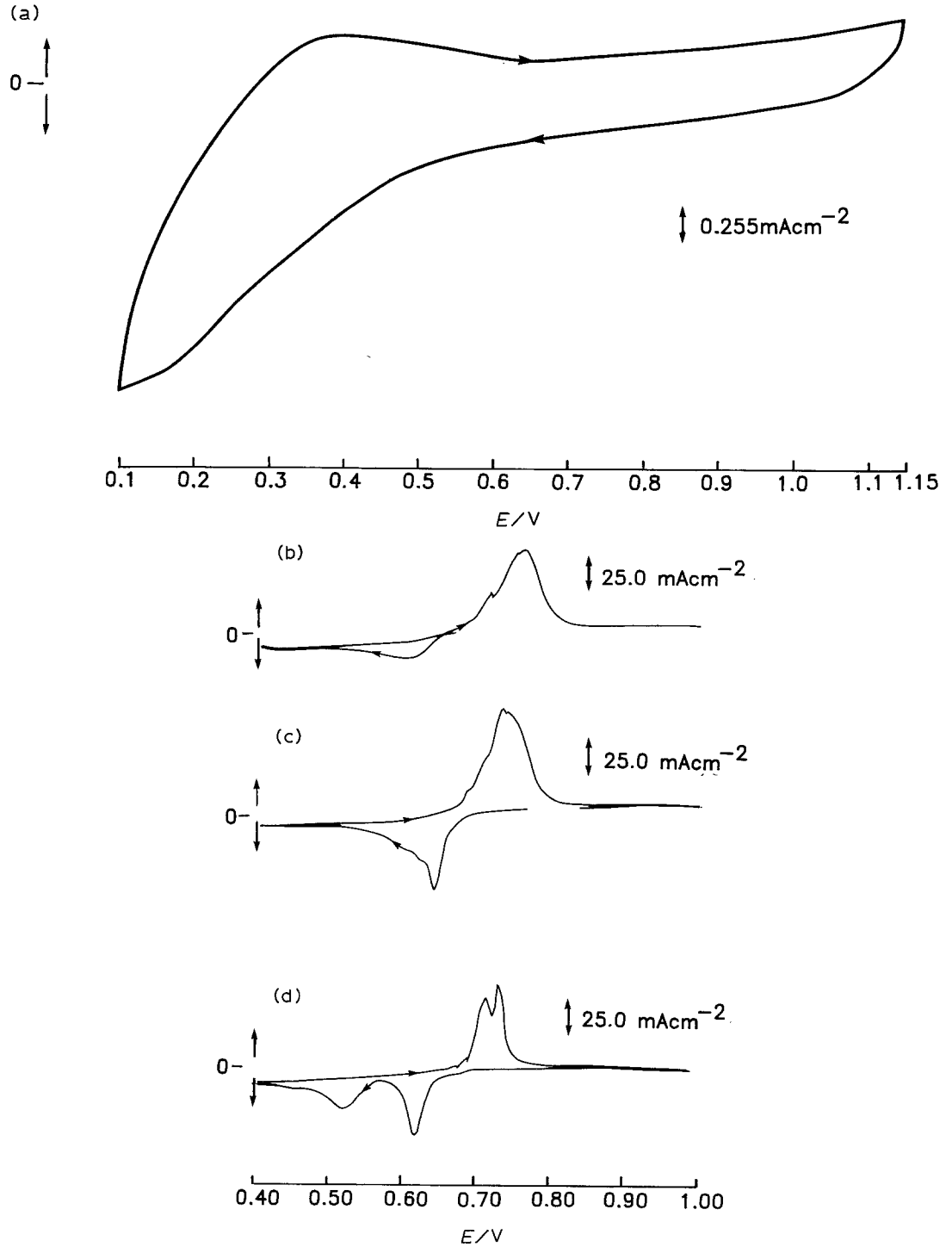

Fig. 5. CV of a tungsten electrode in the NaCl-saturated molten salt in the absence (a) and presence (b–d) of $FeCl_2$; temperature 250 °C, sweep rate 50 mV s^{-1}. (a) Blank; (b) first cycle on a fresh electrode; (c) second cycle; (d) tenth cycle.

sequent cycles, Fig. 5(c). As with the iron electrode, it appears that solid products deposit on the electrode and accumulate during cycling resulting in larger CV currents. Thus, on the first cycle the cathodic peak arises from diffusion of dissolved Fe(II) to the electrode, giving rise to a broad diffusion peak; on subsequent cycles solid $FeCl_2$ and/or Na_6FeCl_8 is reduced in preference. The CVs obtained on tungsten were often noisy and unpredictable, probably due to poor contact between the deposited iron-containing film and the substrate. However, in some cycles, two sharp anodic peaks, separated by about 20 mV, can be clearly discerned (Fig. 5(d)). These observations are fully consistent with the CVs of Figs 2 and 4.

Our general interpretation of voltammograms such as those of Figs 2, 4 and 5 suggests that both solid and solution phase reagents are involved. The sharp doublets appear to be due to the involvement of solid surface layers in redox processes, while the broader, wider spaced anodic and cathodic peaks arise from diffusion of dissolved reagents (e.g. Cl^- and $FeCl_4^{2-}$) to the electrode surface.

The fine structure seen in the various voltammograms almost certainly involves the solid intermediate Na_6FeCl_8 in reactions such as Reactions 3,–3 and 4,–4. The two stage charging and discharging via this compound gives rise to a 12–13 mV step in the open circuit voltage which has been seen both in full sized cells [2] and in small capacity cathodes [13] (see also Section 3.4 below). According to Reactions 3 and 4, the electric charges involved in the two stages are in the ratio 3 : 1. The CV peaks in Fig. 2 are not fully resolved, but a ratio of this order would seem reasonable.

The positions and spacing of the peaks seen in Figs 4 and 5 do not match exactly. Among the possible contributing factors, it is possible that there may be variations of the order of 10–20 mV in the potential of the reference electrode. However, the voltammograms show clear indications that resistive (*IR*) effects could be very substantial. In this connection, the irregular behaviour of the voltammograms on tungsten has been referred to above. More subtle *IR* effects are also evident in voltammograms at iron electrodes. For example, the main cathodic peak in Fig. 4(a) shifts by about 17 mV during cycling, as the peak height changes. Between Fig. 4(c) and (d), the main anodic peak potential shifts by a similar amount. These discrepancies could not be due to reference electrode errors. They clearly do correlate with peak currents, and can readily be explained in terms of the *IR* drop across solid surface films. Thicker films produce higher peak currents and greater potential shifts.

Osteryoung and coworkers have reported voltammetric studies on solutions of Fe^{3+} in a 1 : 1 melt [21]. Under appropriate conditions they noted two closely-spaced anodic peaks which were attributed to the oxidation of Fe to $FeCl_2$. Their interpretation of the double peak hinged on the availability of dissolved Cl^- near the electrode surface; with the benefit of hindsight, it now appears that the two peaks arise from the two-step oxidation, involving the intermediate Na_6FeCl_8, mentioned above.

CVs measured at temperatures above 250 °C differed from those discussed above in a number of important respects. Examples are shown in Fig. 6. With these CVs, there was no build up of the peaks during continuous cycling. Also, the cathodic peak areas are significantly less than the anodic areas, indicating poor coulombic reversibility. The onset of anodic current is in the form of a gradual increase, culminating in a sharp peak before passivation occurs. The first cathodic process seen on the cathodic sweep in Fig. 6(a) gives a sharp peak, followed by a broader peak which appears to arise from solution diffusion. Finally, although the CVs are complex, they lack some of the detail which is evident at lower temperatures. The enhanced

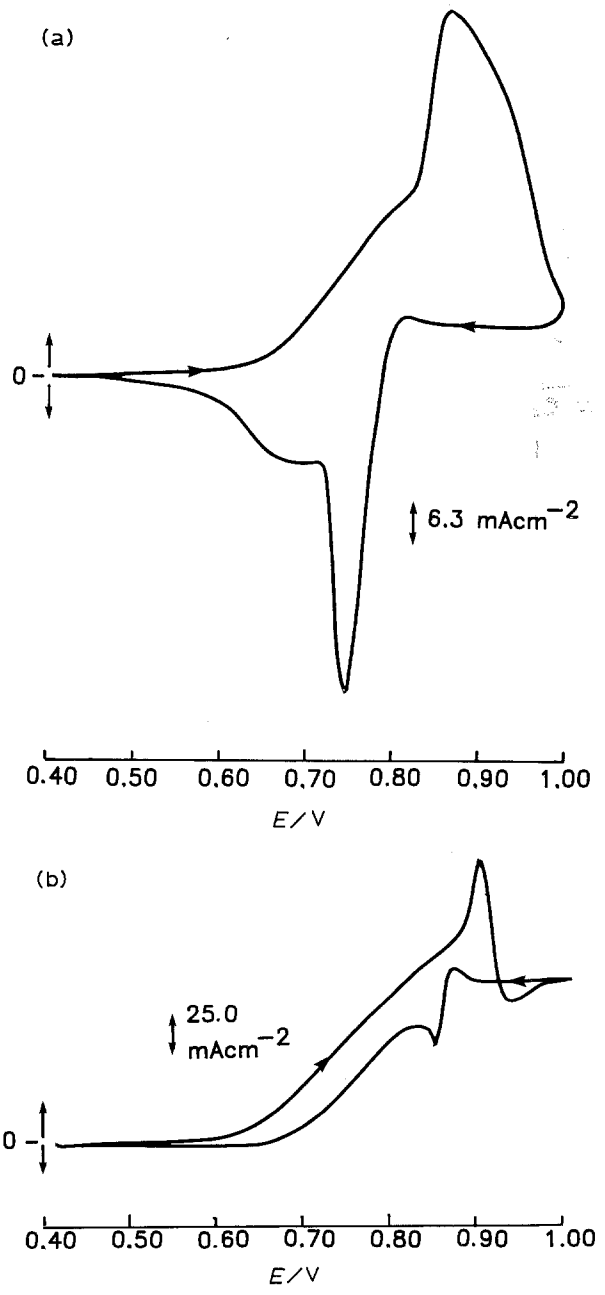

Fig. 6. CVs of an iron wire in the molten salt at elevated temperatures, sweep rate 50 mV s^{-1}. (a) 300 °C; (b) 375 °C.

solubility of $FeCl_2$ as the temperature increases is clearly a major factor in the changing pattern of the CVs above 250 °C. With little or no solid $FeCl_2$ present at the start of the cathodic phase of the CV, deposition of solid NaCl will also be minimal. Solution phase reagents and products thus dominate these CVs, although some sharp features do remain, suggesting the participation of solid reactive films. It is perhaps significant that the most favourable cathodic (i.e. discharge) process does appear from the peak shapes to be solid state in nature. The apparent sluggishness of the first anodic process is also noteworthy; this is presumably the oxidation of iron in the presence of dissolved Cl^- to form $FeCl_4^{2-}$.

Under certain conditions, an unusual oscillatory type of CV was observed. Specifically, during continuous potential cycling of an iron wire electrode in the melt, the current response alternated regularly between two similar, but clearly distinct, patterns. This alternating pattern continued indefinitely. The phenomenon was observed during experiments of the type shown in Fig. 4, where the potential limits of the CV were varied during continuous cycling. For example, at 300 °C, cycling of the iron electrode at 50 mV s^{-1} between limits of 0.40 and 1.00 V gives rise to a normal steady state voltammogram, Fig. 6(a). When the cathodic limit is changed to 0.76 V, the first few cycles show apparently chaotic behaviour (Fig. 7(a)), but the pattern soon resolves itself into two distinct, alternating voltammograms, Fig. 7(b). The final, steady state pattern corresponds to a situation where the current response varies regularly with a period which is twice that of the potential.

Periodic variations in chemical reaction rates are well known [22], and particular cases have been reported which involve the anodic dissolution of metals [23–26]. The latter examples involve either constant potential conditions [23–25] or a slowly changing potential [26], accompanied by periodic current oscillations. There do not appear to be previous examples of electrochemical periodicity of the type reported here, though the underlying reasons in the present case are almost certainly analogous to those in the cases cited above. The anodic oxidation of gold in chloride media exhibits current oscillations as a result of competition between dissolution of the gold as $AuCl_2^-$ (which depletes the local Cl^- concentration) and formation of a passivating layer of gold hydroxide (which leads to a decrease in current and a recovery on the local Cl^- concentration) [23]. Similar oscillations arise in the Cu/Cl^- system with the periodic growth and dissolution of a surface film of solid CuCl [24,25].

The investigation of the oscillations in this molten salt system was limited to a brief survey of the range of conditions under which the oscillations were observable. Periodic behaviour was only seen in the temperature range of 290–310 °C. At 300 °C, and with an anodic potential limit of 1.00 V, the sweep rate needed to be between 50 and 100 mV s^{-1}, and

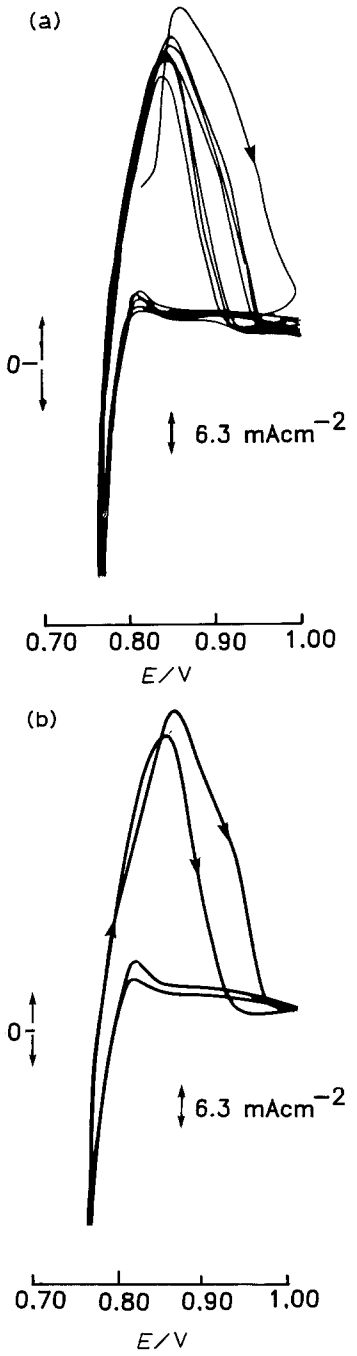

Fig. 7. CVs of an iron wire in the molten salt at 300 °C showing oscillatory behaviour. (Figure 6(a) shows normal voltammogram with sweep limits of 0.400 V and 1.000 V, sweep rate 50 mV s^{-1}.) (a) Pattern observed immediately after switching cathodic limit to 0.760 V; (b) steady state pattern, cathodic limit = 0.760 V.

the cathodic limit in the range 0.760 ± 0.010 V. It appears therefore that the oscillating CV behaviour is confined to a very narrow range of conditions. Figure 7 corresponds to conditions which are close to the optimum for observing the phenomenon.

It is suggested that the periodicity observed in the present system arises from competition between anodic dissolution of iron as a chloride-rich complex such as $FeCl_4^{2-}$, which would deplete the local chloride ion concentration, and the formation of a solid surface film of $FeCl_2$, which would have a passivating effect and would consume less chloride. (In this context $FeCl_2$ is not distinguished from other solid Fe(II)-chloride phases such as Na_6FeCl_8.) It is signifi-

cant that the temperature region where oscillations are observed is intermediate between the low temperature region (where buildup of solids on the electrode surface is important) and the high temperature region of CVs (where dissolution of any deposited solids is very rapid). The relatively small amount of cathodic charge passed in each of the potential cycles indicates that dissolution and diffusion/convection away from the electrode is the major fate of anodically formed Fe(II) under these conditions.

3.3. *Chronopotentiometry*

Current reversal chronopotentiometry was used to obtain quantitative information on the charge passed during oxidation and subsequent reduction of an iron wire electrode at various currents and temperatures. In order to obtain reproducible results, it was found necessary to first carry out repeated, uninterrupted current reversal between the potential limits of 1.00 and 0.40 V. When t_a and t_c (see below) reached constant values, the chronopotentiogram was recorded. A typical example is shown in Fig. 8.

Data from a number of chronopotentiograms are summarized in Table 1. In this table t_a represents the time between the start of the anodic current and the current switching (which was done when the potential reached 1.00 V), while t_c is the time taken, after the current reversal, for the potential to reach the cathodic cutoff of 0.40 V. The final column expresses the coulombic reversibility (t_a/t_c), which is highest at low temperatures and/or high currents (i.e when the experimental timescale is shortest). This is clearly related to dissolution and loss of Fe(II) from the electrode, since formation and retention of solid products during both the current phases would lead to a t_a/t_c ratio of 1.00 at the steady state.

3.4. *Electrochemistry of sintered cathodes*

The charge/discharge behaviour of small sintered Fe–NaCl cathodes has also been studied. In this configuration there tends to be a steady, cumulative capacity loss upon extended cycling [13], but over a limited number of cycles the electrochemical behaviour may still be conveniently studied. Figure 9 shows the potential–time behaviour of an electrode of 101 mAh capacity during charge at a constant current of 10.1 mA. The 12–13 mV step attributed to the solid intermediate Na_6FeCl_8 is clearly evident, even on closed circuit. Also noteworthy is the excess potential required to initiate charging on the two main plateaux. This appears to be due to nucleation overpotential, and presumably relates to the initial formation of solid Na_6FeCl_8 and $FeCl_2$, respectively. X-ray powder diffraction analyses of matched electrodes which had been slowly charged to various extents confirmed that on the lower plateau NaCl is consumed while no $FeCl_2$ is formed. At the position of the step between the plateaux (after about 8200 s), Na_6FeCl_8 is present, but no NaCl or $FeCl_2$. At 80% of capacity both $FeCl_2$ and Na_6FeCl_8 are detectable, and at 100% charge only $FeCl_2$ remains. This is fully consistent with the two stage charge and discharge, Reactions 3,–3 and 4,–4 proposed by Bones and coworkers [2]. The short arrest in the potential seen at about 33 000 s was not readily reproducible, but possibly originates from iron oxidation in the presence of dissolved Cl^-, whereas the lower plateau utilizes solid chloride. This would be in keeping with the interpretation of voltammograms such as Fig. 2.

3.5. *Solid state electrochemical cell*

In view of the strong indications of a solid state mechanism, it was decided to test the solid state cell

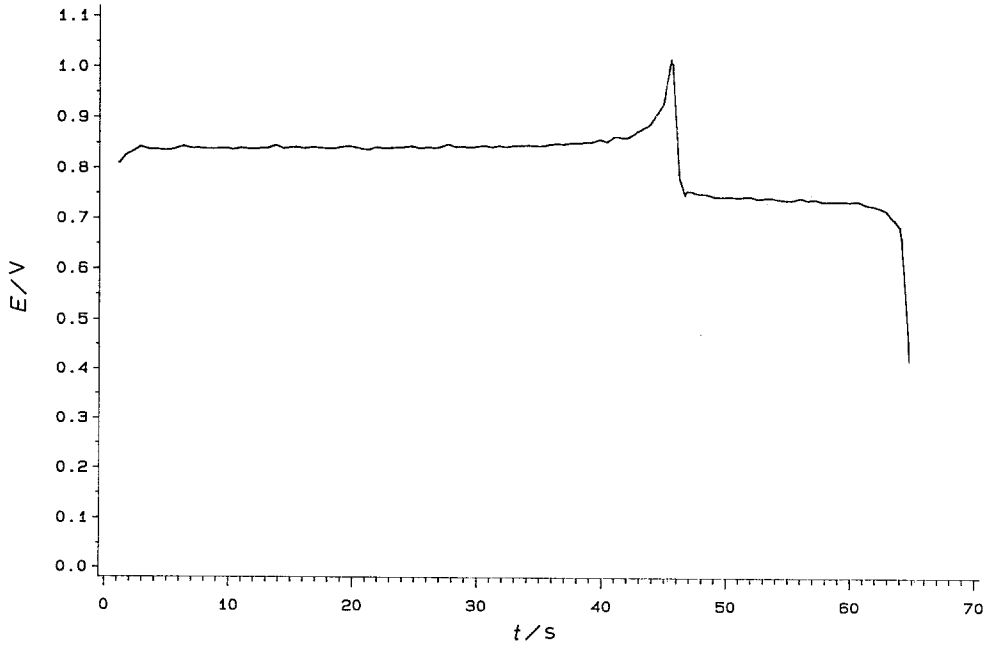

Fig. 8. Current reversal chronopotentiogram of iron wire in the molten salt at 250 °C, current 1.6 mA.

Table 1. Chronopotentiometry of iron wire electrodes

T/°C	I/mA	t_a/s*	t_c/s*	t_a/t_c†
175.0	0.50	81.2	77.3	0.95
175.0	1.00	22.9	22.3	0.97
200.0	1.00	30.0	22.0	0.73
200.0	1.20	21.1	17.3	0.82
250.0	1.40	60.4	23.9	0.40
250.0	1.80	32.9	16.2	0.49
300.0	2.80	62.9	8.6	0.14
300.0	3.50	28.5	7.9	0.28
350.0	4.00	51.9	4.6	0.09
350.0	5.00	22.1	4.4	0.20

*t_a and t_c are anodic and cathodic transition times.
†t_a/t_c is the coulombic reversibility.

described in the experimental section. On charge, the negative electrode was always iron; the positive electrode disc was either iron, nickel or copper. The cell was operated at 290 °C, since it was found that larger charging currents could be achieved at this temperature than at 250 °C. After constant voltage charging, the cell was open circuited and the cell e.m.f. was then monitored using a high impedance digital voltmeter. Relevant cell reactions and calculated e.m.f.s [16] for the charged cells are as follows:

$$2Na(l) + FeCl_2(s) \rightarrow Fe(s) + 2NaCl(s) \quad (E = 2.34\,V) \quad (1)$$

$$2Na(l) + NiCl_2(s) \rightarrow Ni(s) + 2NaCl(s) \quad (E = 2.60\,V) \quad (7)$$

$$2Na(l) + CuCl_2(s) \rightarrow Cu(s) + NaCl(s) \quad (E = 2.34\,V) \quad (8)$$

For the Na–$FeCl_2$ cell, charging was performed at either 2.75 or 3.00 V; typical currents observed were $\sim 0.1\,\mu A$. After extended charging (up to 18 h) an open circuit cell e.m.f. of 2.24 V was measured, only 0.10 V below that calculated for Reaction 1. This e.m.f. was stable for about 10 min, after which it began to fall slowly. The nickel cell was charged at 3.00 V for 18 h, with similar currents to those seen on the iron cell. An e.m.f. of 2.42 V, stable for 30–45 s, was then measured. Once again the e.m.f. is close to the theoretical value, lending further support to the existence of a solid state mechanism for charge and discharge.

The copper cell gave somewhat ambiguous results. When it was charged at 3.50 V, an initial current of $\sim 10\,\mu A$ was observed which increased rapidly over a 15 min period. This behaviour suggests a developing short circuit. After 1 min at open circuit, the measured e.m.f. was steady at 0.98–1.00 V, much less than the calculated value for Reaction 8. It is possible that no sodium metal accumulated during charging, and that the observed voltage in fact corresponds to the e.m.f. of the cell

$$Fe(s) + 2CuCl_2(s) \rightarrow FeCl_2(s) + 2CuCl(s) \quad (9)$$

for which an e.m.f. of 1.21 V is predicted [16].

The poor performance of the solid state cells could be due to a number of causes: the relatively large NaCl particles present, their poor ionic conductivity, inadequate electrical contact at the metal–salt interface, and the substantial distance over which ions must migrate between the electrodes. The NaCl particles present in a normal cathode after several cycles

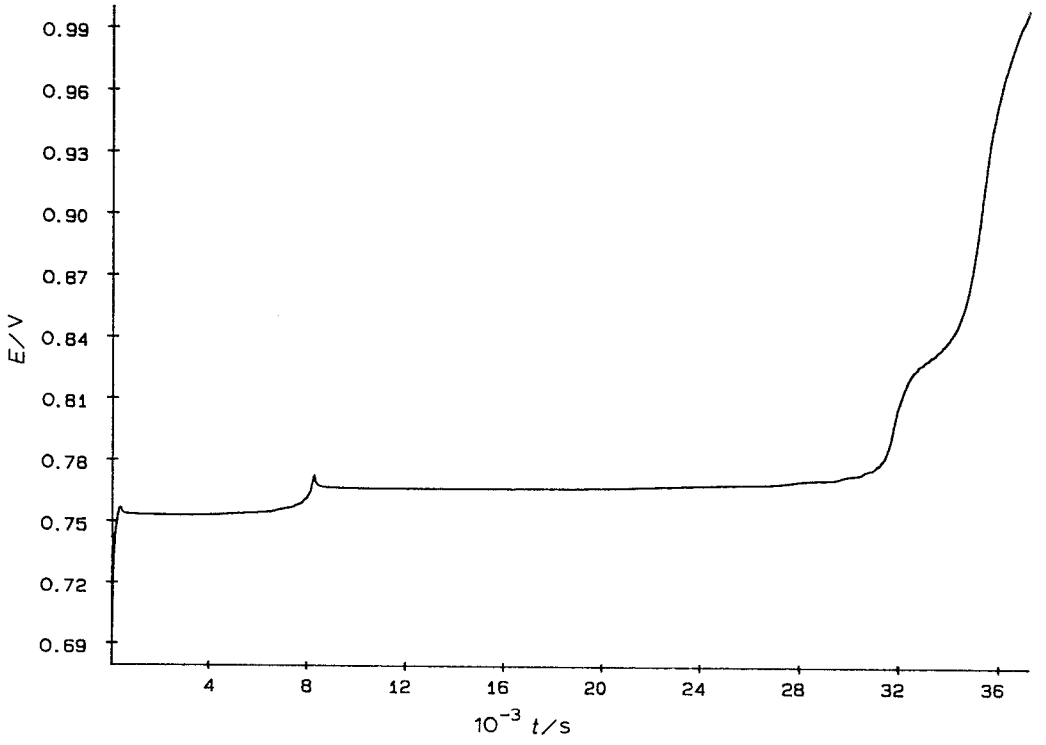

Fig. 9. Potential against time behaviour for slow charging of a sintered Fe–NaCl electrode at 250 °C. Electrode capacity 101 mAh (based on solid NaCl), current 10.1 mA. Dimensions: cylindrical length ~ 6 mm, diameter 7 mm.

would be much smaller than 20 μm, and the presence of any defects and impurities would improve their conductivity and facilitate a solid state mechanism for charge and discharge.

4. Summary

The current buildup in CVs of iron wires at 250 °C clearly demonstrates the importance of solid surface deposits of NaCl and $FeCl_2$ in enhancing the charge and discharge capacity of the electrodes. CV has also shown that the oxidation and reduction of such electrodes, on which solid salts have been deposited, each involve at least three separate important processes. For both the oxidation and reduction there appears to be one process involving solution species and two solid state reactions. The latter are separated in potential by 20–40 mV, and correspond to Reactions 3,–3 and 4,–4, whose equilibrium separation is 12–13 mV [2, 13]. The solid compound Na_6FeCl_8 is confirmed as an intermediate in both the charge and discharge reactions, but does not appear to have any serious adverse effect on the kinetics. At this temperature, the normal cell operating temperature, the solid state reactions are favoured over the reactions of dissolved species.

At temperatures above 250 °C, the evidence points to the increasing importance of dissolution of solid products, and to the participation of dissolved reagents in the redox chemistry. In contrast to a bare wire electrode is the situation in a practical, three-dimensional, porous cathode where only a small fraction of the available reagent salts (NaCl and $FeCl_2$) can be in solution at any time. In the presence of these solids, the solid state reactions are likely to retain their importance in the charge and discharge processes.

The relative contributions of solid and solution phase reactions in an operating cathode will also be expected to depend on the rates of charge and discharge employed, which would strongly influence the local overpotentials. The CV results at 250 °C suggest that at moderate overpotentials the solid state processes are favoured, whereas at more extreme overpotentials the reactions of solution species will gain in importance.

The enhanced solubility of NaCl and $FeCl_2$ at high temperatures could lead to problems in cathode performance arising from the diffusion and migration of reagents within the cathode. Such transportation could, for example, lead to segregation of the Fe and NaCl reagents in the discharged cathode, and to breakdown of electrical continuity through loss of contact in the electronically conducting Fe backbone or blocking of the electrolyte-filled pores. Effects such as these could well be responsible for the reported capacity losses which can occur in full sized cathodes when cells are operated at temperatures in excess of 300 °C [27].

Acknowledgements

We thank the University of the Witwatersrand and the Foundation for Research Development for financial support.

References

[1] J. Coetzer, *J. Power Sources* **18** (1986) 377.
[2] R. J. Bones, D. A. Teagle, S. D. Brooker, F. L. Cullen and J. Lumsdon, 'The Electrochemical Society Extended Abstracts', Vol. 87-1, Philadelphia, PA, 10–15 May (1987) Abstract 553, p.786.
[3] R. C. Galloway, *J. Electrochem. Soc.* **134** (1987) 256.
[4] R. J. Bones, J. Coetzer, R. C. Galloway and D. A. Teagle, *ibid.* **134** (1987) 2379.
[5] J. L. Sudworth, *Chemistry and Industry* (1988) 77.
[6] K. T. Adendorff and M. Thackeray, *J. Electrochem. Soc.* **135** (1988) 2121.
[7] R. J. Bones, D. A. Teagle, S. D. Brooker and F. L. Cullen, *ibid.* **136** (1989) 1274.
[8] P. T. Moseley, R. J. Bones, D. A. Teagle, B. A. Bellamy and R. W. M. Hawes, *ibid.* **136** (1989) 1361.
[9] L. Redey and D. R. Vissers, 'The Electrochemical Society Extended Abstracts', Vol. 89–2, Hollywood, FL, 15–20 October (1989) Abstract 95, p. 143.
[10] I. Bloom, S. K. Orth and D. R. Vissers, 'The Electrochemical Society Extended Abstracts', Vol. 89–2, Hollywood, FL, 15–20 October (1989) Abstract 96, p. 145.
[11] B. V. Ratnakumar, S. di Stefano and G. Halpert, *J. Electrochem. Soc.* **137** (1990) 2991.
[12] S. W. Orchard and G. Mamantov, *ibid.* **136** (1989) 3565.
[13] J. S. Weaving and S. W. Orchard, *J. Power Sources* **36** (1991) 537.
[14] G. Torsi and G. Mamantov, *Inorg. Chem.* **10** (1971) 1900.
[15] L. G. Boxall, H. L. Jones and R. A. Osteryoung, *J. Electrochem. Soc.* **120** (1973) 223.
[16] (*a*) I. Barin and O. Knacke, 'Thermochemical Properties of Inorganic Substances', Springer Verlag, Berlin (1973).
(*b*) I. Barin, O. Knacke and O. Kubaschewski, 'Thermochemical Properties of Inorganic Substances – Supplement', Springer Verlag, Berlin (1977).
[17] R. S. Nicholson and I. Shain, *Anal. Chem.* **36** (1964) 706.
[18] A. J. Bard and L. R. Faulkner, 'Electrochemical Methods', Wiley, New York (1980) Chapter 6.
[19] D. J. Schiffrin, *J. Electroanal. Chem.* **201** (1986) 199.
[20] R. D. Hancock, private communication (1989).
[21] L. G. Boxall, H. L. Jones and R. A. Osteryoung, *J. Electrochem. Soc.* **121** (1974) 212.
[22] R. J. Field and M. Burger (Eds.), 'Oscillations and Travelling Waves in Chemical Systems', Wiley, New York (1985).
[23] J. J. Podesta, R. C. V. Piatti and A. J. Arvia, *Electrochim. Acta* **24** (1979) 633.
[24] R. S. Cooper and J. H. Bartlett, *J. Electrochem. Soc.* **105** (1958) 109.
[25] M. R. Bassett and J. L. Hudson, *ibid.* **137** (1990) 922.
[26] O. Teschke and D. M. Soares, *ibid.* **136** (1989) 1985.
[27] R. J. Wedlake, private communication (1990).